Heat Mass Transfer
DOI 10.1007/s00231-016-1871-9

ORIGINAL

# An investigation of thermal performance improvement of a cylindrical heat pipe using $Al_2O_3$ nanofluid

**M. Ghanbarpour[1,2] · R. Khodabandeh[1] · K. Vafai[2]**

Received: 18 January 2016 / Accepted: 11 July 2016


**Abstract** In this study, effect of $Al_2O_3$ nanofluid on thermal performance of cylindrical heat pipe is investigated. An analytical model is employed to study the thermal performance of the heat pipe utilizing nanofluid and the predicted results are compared with the experimental results. A substantial change in the heat pipe thermal resistance, effective thermal conductivity and entropy generation of the heat pipe is observed when using $Al_2O_3$ nanofluid as a working fluid. It is found that entropy generation in the heat pipe system decreases when using a nanofluid due to the lower thermal resistance of the heat pipe which results in an improved thermal performance. It is shown that the proposed model is in reasonably good agreement with the experimental results and can be used as a fast technique to explore various features of thermal characteristics of the nanofluid based heat pipe.

**List of symbols**

| | |
|---|---|
| h | Convective heat transfer coefficient (W/m$^2$ K) |
| $h_{fg}$ | Latent heat of the working fluid (KJ/Kg) |
| k | Thermal conductivity (W/mK) |
| $k_{eff}$ | Effective thermal conductivity of the wick (W/mK) |
| L | Length of the heat pipe (m) |
| $L_c$ | Length of the condenser section (m) |
| $L_a$ | Length of the adiabatic section (m) |
| $L_e$ | Length of the evaporator section (m) |
| P | Pressure (Pa) |
| Q | Input heat (W) |
| $R_v$ | Vapor core radius (m) |
| $R_o$ | Heat pipe's outer radius (m) |
| $R_w$ | Heat pipe's inner radius (m) |
| S | Entropy (J/K) |
| $T_h$ | Heat source temperature (K) |
| $T_l$ | Heat sink temperature (K) |
| $v_1$ | Vapor injection velocity (m/s) |
| $v_2$ | Vapor suction velocity (m/s) |

**Greek symbols**

| | |
|---|---|
| $\varepsilon$ | Porosity of the wick (%) |
| $\rho$ | Density (kg/m3) |
| $\mu$ | Dynamic viscosity (Pa.s) |

**Subscripts**

| | |
|---|---|
| *l* | Liquid phase |
| *v* | Vapor |
| *nf* | Nanofluid |
| *p* | Particle |
| *s* | Solid |

**Superscript**

| | |
|---|---|
| + | Dimensionless quantity |

## 1 Introduction

As the industrial technologies upgrade continuously, the need for efficient cooling techniques is becoming more important and inevitable. Among different cooling technologies, two phase heat transfer devices have several attractive features. Heat pipe as a two phase heat transfer device, with high flexibility and effective thermal performance, plays a vital role in many industrial applications

✉ K. Vafai
vafai@engr.ucr.edu

[1] Department of Energy Technology, Royal Institute of Technology, 100 44 Stockholm, Sweden

[2] Department of Mechanical Engineering, University of California, Riverside, CA 92521-0425, USA

Published online: 21 July 2016

like cooling of electronic components, aerospace, power generation, chemical processes and heat exchanger applications. In a heat pipe system, a large amount of heat can be transferred with a relatively low temperature drop along the heat pipe due to double phase change and capillary action for pumping the liquid through a porous material. Thermal performance of a heat pipe is linked to the selection of working fluid since the properties of the working fluid affects the heat transfer capability and capillary action. A traditional heat transfer fluid like water is widely used in heat pipes, but, it is desirable to enhance its thermal properties as it has a significant effect on thermal performance of the heat pipe and its heat removal capability. For heat transfer applications, using a nanofluid is a desirable solution as thermal properties such as higher thermal conductivity and critical heat flux can be exploited by nanofluids [1–8]. In recent years, researchers have investigated the thermal performance of heat pipes using nanofluids with different nanoparticles types and morphologies [9–16]. Liu and Zhu [17] experimentally investigated the thermal performance of a horizontal mesh heat pipe using aqueous CuO nanofluid. They reported 60 % reduction of the thermal resistance at 1 wt % CuO nanofluid. Wang et al. [18] studied effects of CuO nanofluids on thermal performance of a cylindrical miniature grooved heat pipe. Their results revealed that the maximum heat flux and evaporator heat transfer coefficient increased by 35 and 100 %, respectively. Asirvatham et al. [19] performed experiments to investigate the effect of Ag nanofluid on the thermal performance of a screen mesh heat pipe. Based on their experiments, thermal resistance of the heat pipe decreased by 76 % at volume concentration of 0.009 % compared with water. Do et al. [20] carried out an experiment to study the heat transfer performance of a screen mesh heat pipe using $Al_2O_3$ nanofluid. They reported a 40 % reduction of thermal resistance at the evaporator-adiabatic section at volume concentration of 3 %. Huminic et al. [21] conducted a study to investigate the effect of $Fe_2O_3$ nanofluid on a two phase closed thermosyphon. They found that the thermal resistance decreased by 39 % with nanofluid at volume concentration of 5.3 %. Naphon et al. [22] performed experiments to investigate the effect of $TiO_2$/alcohol nanofluid on an inclined heat pipe. Their experiments showed that the thermal efficiency of the heat pipe increased by 10.6 % at a tilt angle of 45° with nanofluid at a volume concentration of 0.1 %. Gunnasegaran et al. [23] investigated experimentally the effect of $SiO_2$ nanofluid on thermal performance of a looped heat pipe. They reported 28–44 % reduction of the thermal resistance with nanofluid at a volume concentration of 3 % at different heat fluxes. According to the experimental studies, higher thermal conductivity of the nanofluids and the probability of forming a porous layer on the surface of the wick at evaporator section which may improve the capillarity and wettability are the main reasons for the thermal performance improvement of the heat pipes when using the nanofluids. But, the contribution of each phenomenon is not fully scientifically understood.

Although, most of the research work on the thermal performance of a heat pipe using a nanofluid is experimental, there are few works with an analytical focus on modeling heat pipe characteristics in the presence of a nanofluid. A comprehensive analytical model, proposed by Zhu and Vafai [24] and later modified by Shafahi et al. [25], is used for investigation of thermal performance of heat pipes using nanofluids. As the authors stated, the proposed analytical model is quite comprehensive but it is still derived based on some simplifications. For example, the wick is assumed to be fully saturated and the liquid film thickness along the heat pipe is assumed to be constant and unchanged [25]. The changes of the concentration of the nanoparticles at different sections of the heat pipe are neglected. The reason is that at the same rate of the evaporation, the liquid is supplied from condenser through the wick structure. Although some changes in the concentration of the nanoparticles at different sections of the heat pipes are unavoidable, still considering a constant concentration is logical as these changes are quite limited.

The results obtained from the proposed comprehensive analytical method are compared with experimental results. Our intention in this study is to investigate the validity and reliability of the analytical model proposed and reported in the Ref. [25]. The contribution of this study is to provide a clear view regarding the proposed analytical model by comparing the results to the experimental results. In this study, water based $Al_2O_3$ nanofluid at a volume concentration of 1.3 % is used as a working fluid. Thermal resistance, entropy generation and characteristics of wick structure of screen mesh heat pipe are investigated to show nanofluids potential to improve thermal performance of cylindrical heat pipes.

## 2 Analytical analysis

To investigate the effect of a nanofluid as a working fluid on the heat pipe performance, an analytical modification, which was done by Shafahi et al. [25], is employed to calculate temperature and liquid distributions along the heat pipe.

Considering nanofluid as a continuous media with thermal equilibrium between the base fluid and solid nanoparticles, Navier–Stokes equations for steady two-dimensional flow can be solved by integrating momentum equations and applying proper boundary conditions [24]. The liquid and vapor pressure distributions are determined as

**Table 1** Analytical correlations parameter [25]

| | | |
|---|---|---|
| $G_2 = \frac{\mu_{nf}}{2K}\left(B + \frac{1}{\gamma R_v}\frac{2C}{1-\left(\frac{R_w}{R_v}\right)^2}\right)$ | $B = \frac{2R_v}{\rho^+_{nf}(R_w^2 - R_v^2)}\left(1 + \frac{8\rho^+}{\mu^+\gamma^2 R_v^2}\right)$ | $C = \frac{8}{\mu^+_{nf}\gamma R_v^2} - B$ |
| $G = -\frac{\rho_v}{3R_v^2}(D^2 - 7D + 16)$ | $v_1 = \frac{Q}{2\rho_v \pi R_v L_e h_{fg}}$ | $D = CR_v$ |

$$P_l(x) - P_l(0) = \begin{cases} G_2 \upsilon_1 x^2 & 0 \le x \le L_e \\ G_2 \upsilon_1 L_e(2x - L_e) & L_e \le x \le L_e + L_a \\ -G_2 \upsilon_2\left[(x-L)^2 - (L + L_a)L_c\right] & L_e + L_a \le x \le L_e + L_a + L_c \end{cases} \quad (1)$$

$$P_v(x) - P_v(0) = \begin{cases} \left(G\upsilon_1^2 + M\upsilon_1\right)x^2 & 0 \le x \le L_e \\ \left(G\upsilon_1^2 - M\upsilon_1\right)L_e^2 + 2M\upsilon_1 L_e x & L_e \le x \le L_e + L_a \\ \left(G\upsilon_2^2 - M\upsilon_2\right)(x-L)^2 + M\upsilon_2(L + L_a)L_c & L_e + L_a \le x \le L_e + L_a + L_c \end{cases} \quad (2)$$

where $\upsilon_1$ and $\upsilon_2$ are vapor injection and suction velocities, respectively. It is noted that the vapor suction velocity is determined by the mass balance in the vapor region. Other parameters which are used in the analytical correlations, Eqs. 1 and 2, are shown in Table 1.

To determine the wall temperature distribution Zhu and Vafai [24] used a heat conduction model for the wall and wick regions. Employing proper boundary conditions, the heat pipe temperature profile can be presented as follow,

$$T_{wall}(x) = \begin{cases} T_b + \frac{Q}{2\pi L_c}\left[\left(\frac{\ln\left(\frac{R_o}{R_w}\right)}{k_{wall}} + \frac{\ln\left(\frac{R_w}{R_v}\right)}{k_{eff}}\right)\left(1 + \frac{L_c}{L_e}\right) + \frac{1}{hR_o}\right] & 0 \le x \le L_e \\ T_b + \frac{Q}{2\pi L_c}\left[\frac{\ln\left(\frac{R_o}{R_w}\right)}{k_{wall}} + \frac{\ln\left(\frac{R_w}{R_v}\right)}{k_{eff}} + \frac{1}{hR_o}\right] & L_e \le x \le L_e + L_a \\ T_b + \frac{Q}{2\pi L_c h R_o} & L_e + L_a \le x \le L_e + L_a + L_c \end{cases} \quad (3)$$

where $Q$, $h$ and $T_b$ are heat input, convective heat transfer coefficient and bulk temperature of the coolant at heat sink. The effective thermal conductivity of the porous layer, $k_{eff}$, is defined as:

$$k_{eff} = \frac{k_{nf}\left[(k_{nf} + k_s) - (1-\varepsilon)(k_{nf} - k_s)\right]}{(k_{nf} + k_s) + (1-\varepsilon)(k_{nf} - k_s)} \quad (4)$$

where $\varepsilon$, $k_{nf}$ and $k_s$ are porosity, thermal conductivities of the nanofluid and solid matrix, respectively.

The wall temperature profile and pressure drops, obtained analytically, can be employed to determine entropy generation in the heat pipe. According to the second law of thermodynamics, there are different sources of entropy generation due to irreversibility occurring inside the heat pipe including friction and transfer of energy over a finite temperature difference.

Entropy generation caused by temperature differences between the vapor and external reservoirs as well as vapor and liquid pressure drops during the process can be presented in the following form.

*Entropy generation due to heat transfer* [26, 27]:

$$S_{HT} = \oint \frac{\delta Q}{T} = \frac{-Q}{T_h} + \frac{Q}{T_l} = Q\left(\frac{T_h - T_l}{T_h T_l}\right) = \frac{Q^2 \cdot R}{T_h(T_h - Q \cdot R)} \quad (5)$$

where $T_h$, $T_l$ and $R$ are heat source and heat sink temperatures and the overall thermal resistance of the heat pipe which is defined as

$$R_{total} = \frac{T_h - T_l}{Q} \quad (6)$$

*Entropy generation due to vapor pressure drop* [26, 27]:

Entropy generation due to the vapor flow friction can be formulated as

$$\mathrm{S_{vapor}} = \frac{\mathrm{m} \cdot \Delta \mathrm{P_{vapor}}}{\rho_\mathrm{v} \cdot \mathrm{T}} \quad (7)$$

where the pressure drop and mass are given by,

$$\Delta \mathrm{P_{vapor}} = \frac{8\mu_\mathrm{v} \cdot \mathrm{V} \cdot \mathrm{L_{eff}}}{\mathrm{R_v^2}} \quad (8)$$

$$m = \frac{Q}{h_{fg}} \quad (9)$$

So,

$$\mathrm{S_{vapor}} = \frac{8\mu_v \cdot V \cdot L_{eff} \cdot Q}{\rho_v \cdot T \cdot R_v^2 \cdot h_{fg}} \quad (10)$$

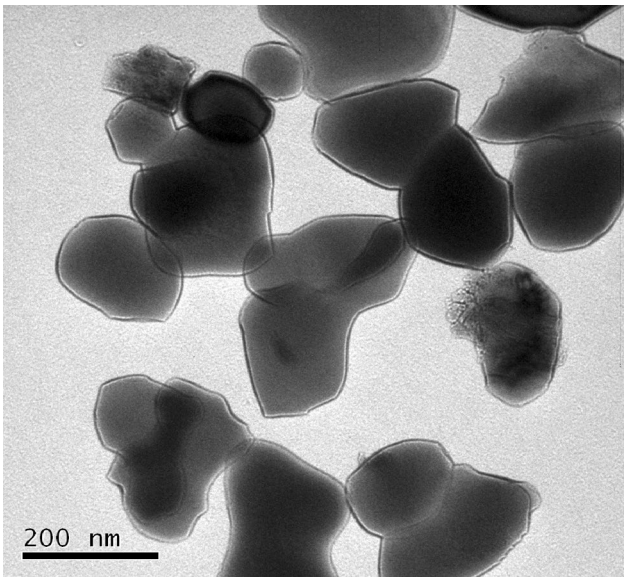


**Fig. 1** TEM images of alumina nanoparticles [29]

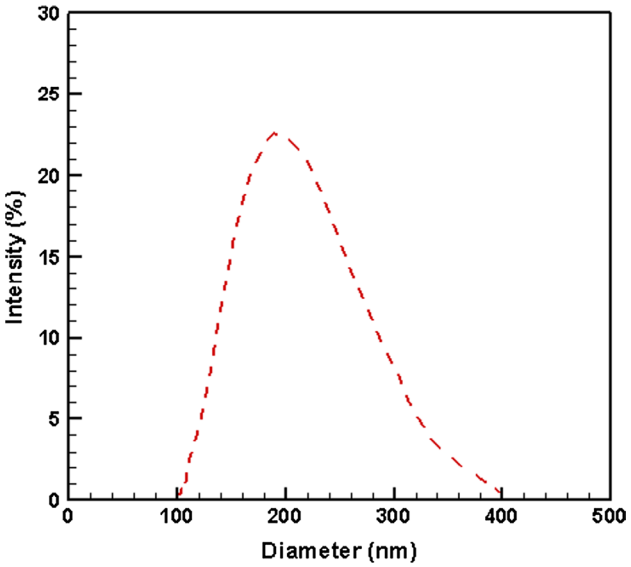


**Fig. 2** Hydrodynamic size distribution of alumina NFs measured by DLS [29]

where $T$, $\rho_v$, $V$, $L_{eff}$, $R_v$ and $h_{fg}$ are temperature, vapor density, velocity, effective length, vapor channel radius and latent heat of vaporization, respectively.

*Entropy generation due to liquid pressure drop* [26, 27]:

Entropy generation due to the liquid flow friction can be formulated as

$$S_{liquid} = \frac{m \cdot \Delta P_{liquid}}{\rho_l \cdot T} \tag{11}$$

where the liquid pressure drop along the wick is

$$\Delta P_{liquid} = \frac{\mu_{nf} \cdot L_{eff} \cdot Q}{\rho_{nf} \cdot h_{fg} \cdot A_{wick} \cdot K_{permeability}} \tag{12}$$

So,

$$S_{liquid} = \frac{\mu_l \cdot L_{eff} \cdot Q^2}{\rho_l^2 \cdot T \cdot h_{fg}^2 \cdot A_{wick} \cdot K_{permeability}} \tag{13}$$

where $K_{permeability}$, $\rho_l$, $\mu_l$ and $A_{wick}$ are the permeability, liquid density, liquid viscosity and wick cross-sectional area, respectively.

In addition to entropy generation analysis, effective thermal conductivity is of particular interest to evaluate the heat pipe's thermal performance. The effective thermal conductivity of the heat pipe is calculated from:

$$K_{eff} = \frac{L_{eff}}{A.R} \tag{14}$$

where $A$ is the total surface area for the heat input in the evaporator section and heat removal in the condenser section of heat pipe and $L_{eff}$ is the effective transport length calculated by [28]:

$$L_{eff} = 0.5L_e + L_a + 0.5L_c. \tag{15}$$

## 3 Experimentation

### 3.1 Nanofluid

In this investigation, water based $Al_2O_3$ nanofluid at volume concentration of 1.3 %, provided by ItN Nanovation AG, was tested while pH value was adjusted to 9.1. The morphology and primary particle size were determined by transmission electron microscopy (TEM) analysis as shown in Fig. 1. In addition, dynamic light scattering (DLS) analysis was performed for determination of hydrodynamic size of the nanoparticles, as shown in Fig. 2. According to TEM images of alumina nanoparticles, the particle size was in the range of 100–200 nm while the curve broadening in Fig. 2 shows that the hydrodynamic particle size distribution for $Al_2O_3$ is between 100 and 400 nm and an average DLS particle size is reported as 235 nm. Dynamic viscosity and thermal conductivity of both the base liquid and nanofluid are measured experimentally using rotating coaxial cylinder viscometer and Transient Plane Source-analyzer, respectively. Thermal conductivity and viscosity of the working fluids are presented in Table 2. Our results reveal that thermal conductivity and viscosity of the nanofluid increases by 4.2 and 19 %, respectively compared with water. Also, it is found that Maxwell and Einstein correlations underestimate thermal conductivity and viscosity of the nanofluid, respectively.

**Table 2** Thermal conductivity and viscosity of working fluid (303 K)

| | Thermal conductivity (W/mK) | | Viscosity (Pa.s) | |
|---|---|---|---|---|
| | Exp. | Maxwell | Exp. | Einstein |
| Basefluid | 0.6155 | – | 0.00079 | – |
| Nanofluid | 0.6415 | 0.6387 | 0.00094 | 0.00082 |

### 3.2 Experimental apparatus and procedure

The heat pipes, used in this study, are made of a copper tube with length of 200 mm and outer diameter of 6.35 mm. Each heat pipe has 2 layers of 150 meshes per inch and aperture size and wire diameter of screen mesh are 0.106 and 0.063 mm, respectively. The evaporator, adiabatic and condenser sections of the heat pipes were 50, 100 and 50 mm long, respectively. To obtain reliable results with a high accuracy, the heat pipes were built, evacuated and filled at Thermacore Co., a heat pipe manufacturer in Europe, as the charge amount and pressure inside the tubes have significant influence on the thermal performance of the heat pipes.

Experimental test facilities, as shown in Fig. 3, consist of a cooling system as a heat sink with constant temperature bath, a pump (Gear pump, MCP-Z, Ismatec, Switzerland) and flow meter (Coriolis flow meter, CMFS015, Micromotion, Netherlands) and a heat source to generate uniform heat including a power supply (DC power supplier, PSI 9080-100, Elektro-Automatik GmbH, Germany) and also a data acquisition system (Agilent 34970A, Malaysia) were used to perform the experiments. Five K-type thermocouples, mounting two thermocouples at the surface of the evaporator, one at the surface of the adiabatic section and the rest at the surface of the condenser section, were used to measure the heat pipes wall surface temperatures.

The cartridge heaters distributed through the copper blocks at the evaporator section to provide uniform heat. Thermal grease is applied on the interfaces between the copper blocks, heat pipe and cartridge heater to assure the good contacts between the copper blocks, heat pipe and cartridge heater. The power level which is supplied via a power supplier is controlled via a power meter. The condenser section of the heat pipe was cooled by re-circulating water in a loop. The temperature and flow rate of the coolant were measured and controlled to investigate the cooling capacity of the system.

## 4 Result and discussion

To investigate thermal performance of heat pipes using a nanofluid, a modified analytical method [25] is employed and the predicted results are compared with the experimental ones. Water and water/$Al_2O_3$ nanofluid at volume concentration of 1.3 % are used as working fluids. To study accuracy of the analytical model, evaporator wall temperature and temperature difference between evaporator and condenser wall surfaces for heat pipes obtained from analytical study are compared with experimental results. Figure 4 shows the evaporator wall temperature at different heat fluxes for heat pipes containing water and nanofluid. The evaporator wall temperature increases with the increasing of the heat flux while the evaporator wall temperature of the heat pipe using $Al_2O_3$ nanofluid is lower than that of the heat pipe using water. In addition, it is observed that the analytical model predicts the evaporator wall temperature with a good accuracy with maximum differences of 1.5

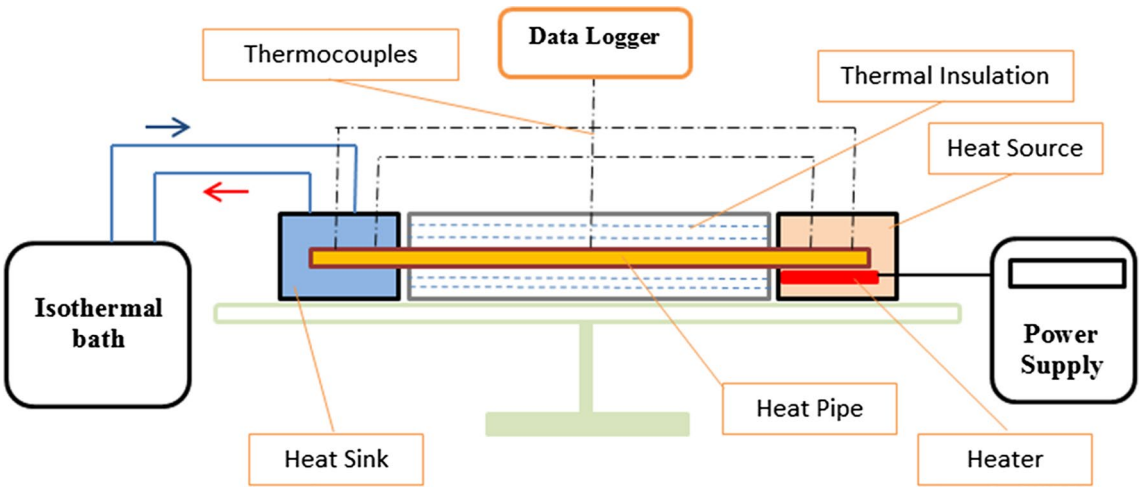


**Fig. 3** Schematic of the experimental apparatus

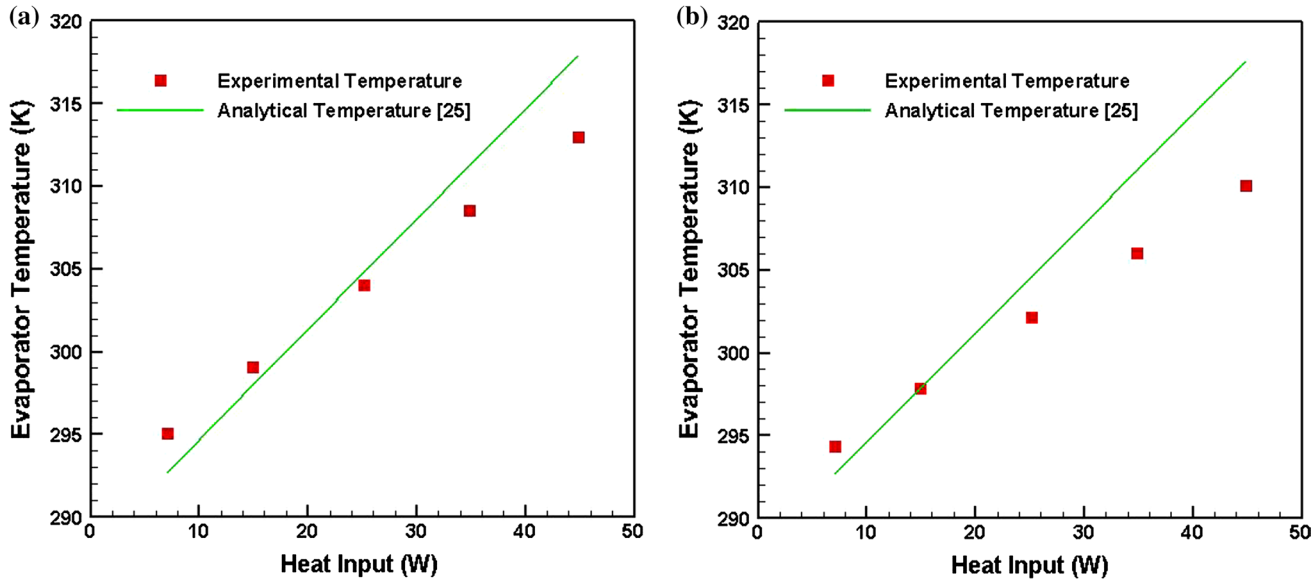


**Fig. 4** Evaporator wall temperature at different heat fluxes for heat pipes with **a** water and **b** nanofluid

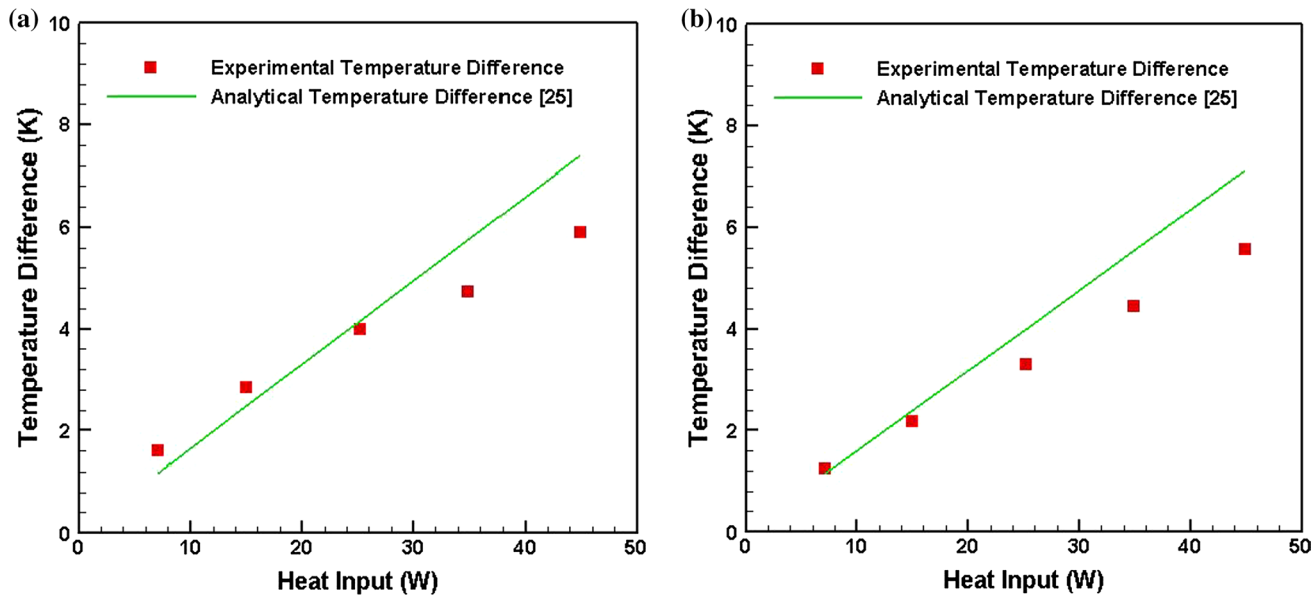


**Fig. 5** Temperature difference between evaporator and condenser wall surfaces for heat pipes with **a** water and **b** nanofluid

and 2.5 % for heat pipes with water and nanofluid, respectively. Figure 5 displays the difference between the evaporator and condenser wall surface temperatures for the heat pipes. Comparing the temperature difference results reveals that the modified analytical model predictions are in good agreement with the experimental results especially at lower heat fluxes. From Eq. 3, it is clear that wall temperatures along the condenser and evaporator sections are uniform. Also, the thermal resistance of heat pipes obtained from analytical model is independent of the heat flux. Figure 6 represents overall thermal resistance of the heat pipes with water and nanofluid. Experimental result reveals that thermal resistance of the heat pipes decreases slightly with an increase in the heat flux at lower heat flux and remains almost constant for most of the heat flux range especially for the heat pipe with a nanofluid. The reason for the reduction of the thermal resistance especially at lower heat load is the higher liquid film thickness at the evaporator which causes a higher partial thermal resistance of the wick. By increasing the heat flux, before the occurrence of dryout,

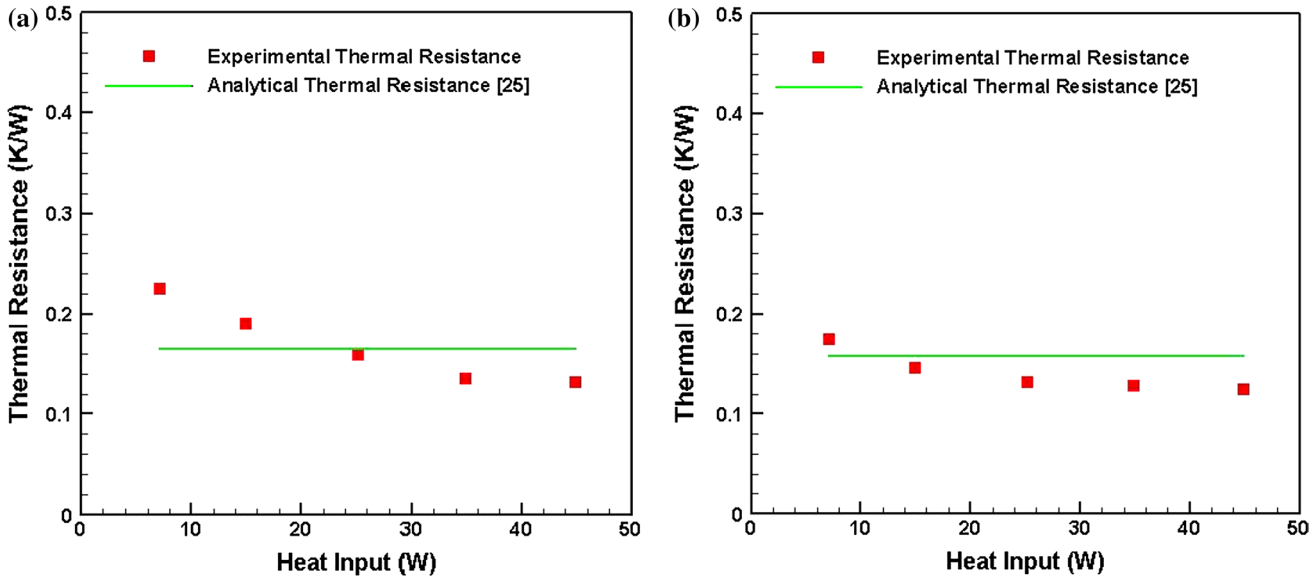


**Fig. 6** Thermal resistance for heat pipes with **a** water and **b** nanofluid

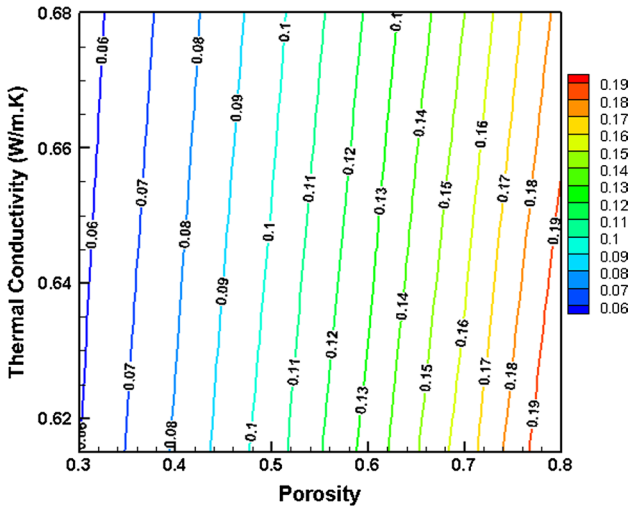


**Fig. 7** Thermal resistance of the heat pipe as a function of porosity of the wick and thermal conductivity of the working fluid

the lowest thermal resistance is observed due to the lower liquid film thickness.

Thermal performance of heat pipes strongly depends on the working fluid properties as well as the heat pipe dimensions and characteristics. According to Eqs. 3 and 4, working fluid thermal conductivity has an influence on the effective thermal conductivity of liquid-wick region. Employing working fluid with higher thermal conductivity results in higher effective thermal conductivity of the porous wick and consequently lower radial conductive resistance. The dependency of the thermal resistance of the heat pipes on the thermal conductivity of the working fluid is shown in Fig. 7. As can be seen, thermal resistance of the heat pipe decreases with an increase in the working fluid thermal conductivity for all wick porosities.

Figure 8 shows thermal resistance as a function of wick porosity and thickness for heat pipes with water and nanofluid. As can be seen, the thermal resistance of both heat pipes increases with an increase of the wick thickness and porosity. An increase in the wick thickness leads to higher radial conductive resistance and the resistance increment is more dominant at higher thicknesses. For instance, for a heat pipe with wick thickness of 0.2 mm, thermal resistance of the heat pipe increases about 3 times when porosity increases from 0.3 to 0.9 while the thermal resistance increase is found to be more than 3.5 times for a heat pipe with wick thickness of 1 mm. In terms of porosity, thermal resistance of the heat pipes increases with an increase in the porosity due to the much higher thermal conductivity of the wick material compared to the thermal conductivity of the working fluid. That is the effective thermal conductivity of the wick increases when the porosity decreases. Average thermal resistance and effective thermal conductivity of the heap pipes are shown in Fig. 9. As can be seen, average thermal resistance of the heat pipes decreases using nanofluid. The probable reasons for the reduction in the thermal resistance of the heat pipe with a nanofluid are the effect on the vapor bubbles during bubble formation by nanoparticles, increasing the wettability and capillary force, increase of heat transfer area in the evaporator by forming a thin porous layer of $Al_2O_3$ particles on the surface of the wick and improvement of effective thermal conductivity of wick [27, 29, 30]. In the analytical method used in this study, nanofluid effects on the two-phase heat

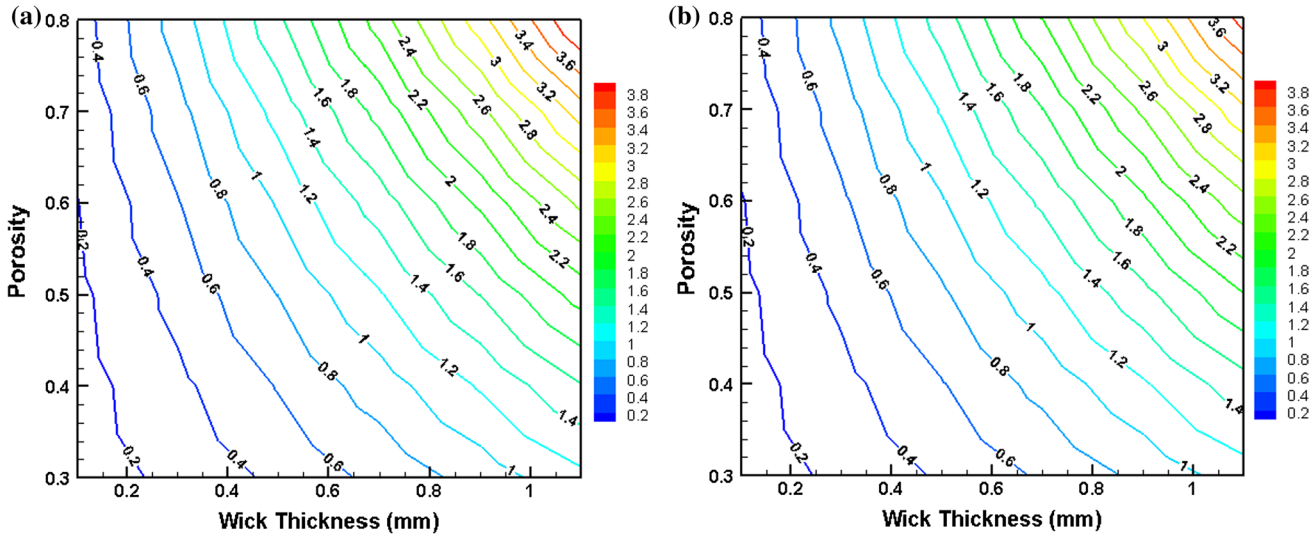


**Fig. 8** Thermal resistance of the heat pipe as a function of porosity and thickness of the wick for heat pipes with **a** water and **b** nanofluid

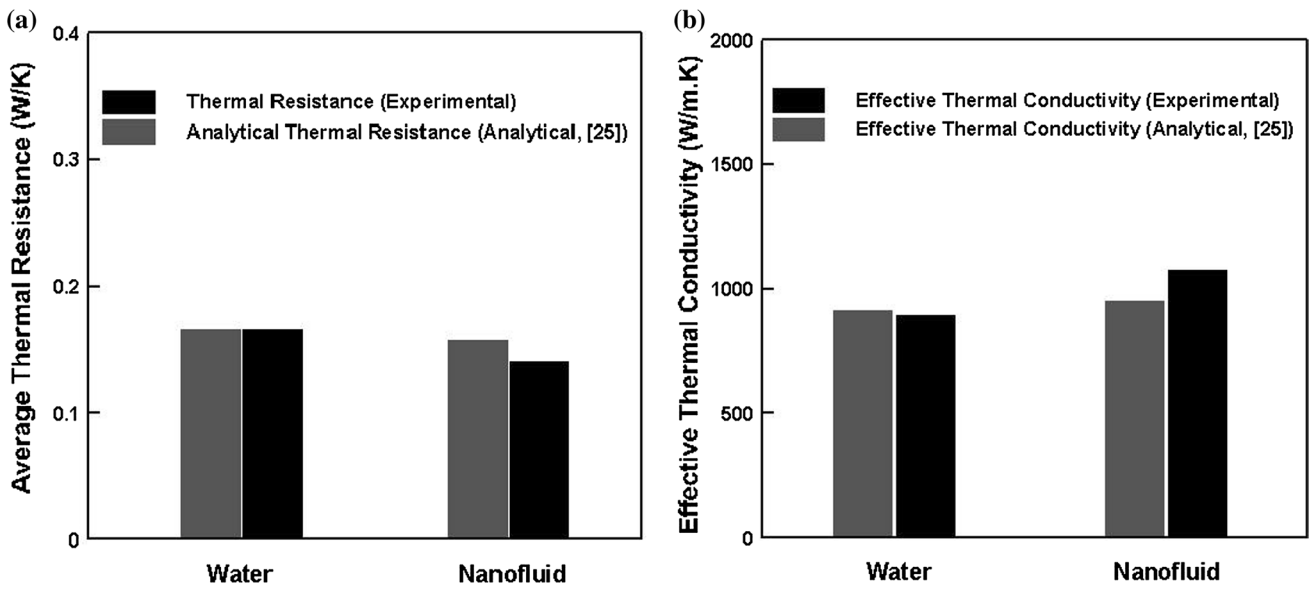


**Fig. 9** Average thermal resistance and effective thermal conductivity of the heat pipes

transfer at liquid–vapor interface is neglected due to the great heat transfer coefficient of the two-phase heat transfer which results in a very low thermal resistance. So, the thermal properties improvement of the nanofluid, in particular thermal conductivity, is taken into account for the wall temperature distribution calculation. Using nanofluid instead of water decreases thermal resistance of the heat pipe by 15 % which shows nanofluid potential to be used as a working fluid in the heat pipe. From Eq. 14, effective thermal conductivity of the heat pipes are calculated as shown in Fig. 9. Results indicate that effective thermal conductivity of the heat pipe increases two to three times in comparison with copper metal rod and can be improved by using nanofluds.

Working fluid properties have an important influence on entropy generation and consequently the amount of lost work during the process. In a heat pipe system, there are different sources of entropy generation such as temperature differences between the vapor and external reservoirs as well as vapor and liquid pressure drops. Liquid pressure drop along the heat pipe is calculated analytically [25] using Eq. 1 and shown in Fig. 10. As can be seen, liquid pressure drop increases using nanofluid as it depends on

liquid viscosity and density. Although both viscosity and density increase by adding particles to a base liquid, these two properties have opposite effect on liquid pressure drop. Higher density results in a lower pressure drop due to the reduction of liquid velocity and shear stress, but, increasing working fluid viscosity leads to higher shear rate and pressure drop along the heat pipe wick. In this study, working fluid viscosity and density increase 1.189 and 1.037 %, respectively. So, in this case, the increase in viscosity overcomes the density effect leading to a larger pressure drop.

Figures 11 and 12 show experimental and analytical entropy generations in heat pipes using water and nanofluid. As expected, Fig. 11 shows that entropy generation increases when the thermal load increases. In addition, as can be seen in Fig. 12, an entropy generation reduction is observed for the heat pipe when using a nanofluid both experimentally and analytically. Although entropy generation due to liquid pressure drop increases with adding particles to the base liquid, the reduction in entropy generation due to heat transfer overcomes the effect of liquid pressure drop. It is due to the great permeability of the heat pipe and some order of magnitude higher latent heat of vaporization than viscosity of the liquid and also the weak effect of the heat flux. An 8 % reduction in average entropy generation indicates that the nanofluid improves the heat pipe performance based on the second law of thermodynamics.

The influence of nanoparticles concentration on the maximum heat load is shown in Fig. 13. As explained by Shafahi et al. [25], there is an optimum nanoparticle concentration level for a nanofluid which is found to be 5 vol% in this study. For the nanoparticle concentration below a critical concentration level, adding the nanoparticles to the base liquid enhances the maximum heat load while after the critical concentration level, the maximum heat load is decreased with an increase in the concentration. The reason for the existence of an optimum nanoparticle concentration level is the opposite roles that density and viscosity have in affecting the maximum heat load. As both density and viscosity increase with an increase in nanoparticle concentration, the opposite role of density and viscosity on the mass flow and pressure loss can result in the existence of an optimum particle concentration level. In addition to that, the higher maximum heat flux at the heat pipe using nanofluid compared to the base liquid is due to the improvement

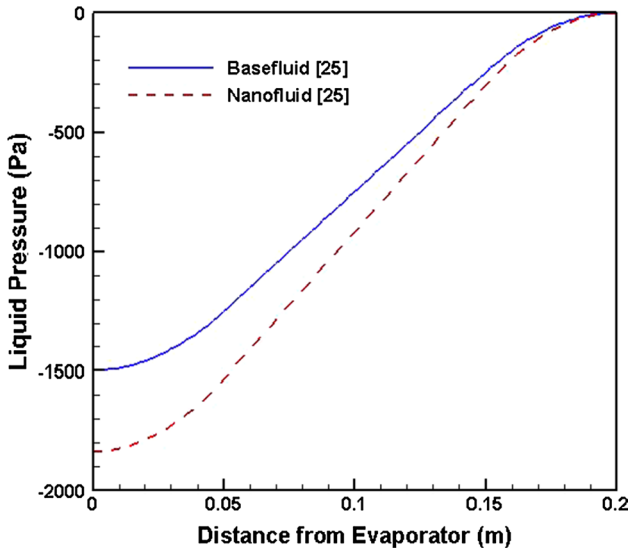


**Fig. 10** Liquid pressure drop along the heat pipe

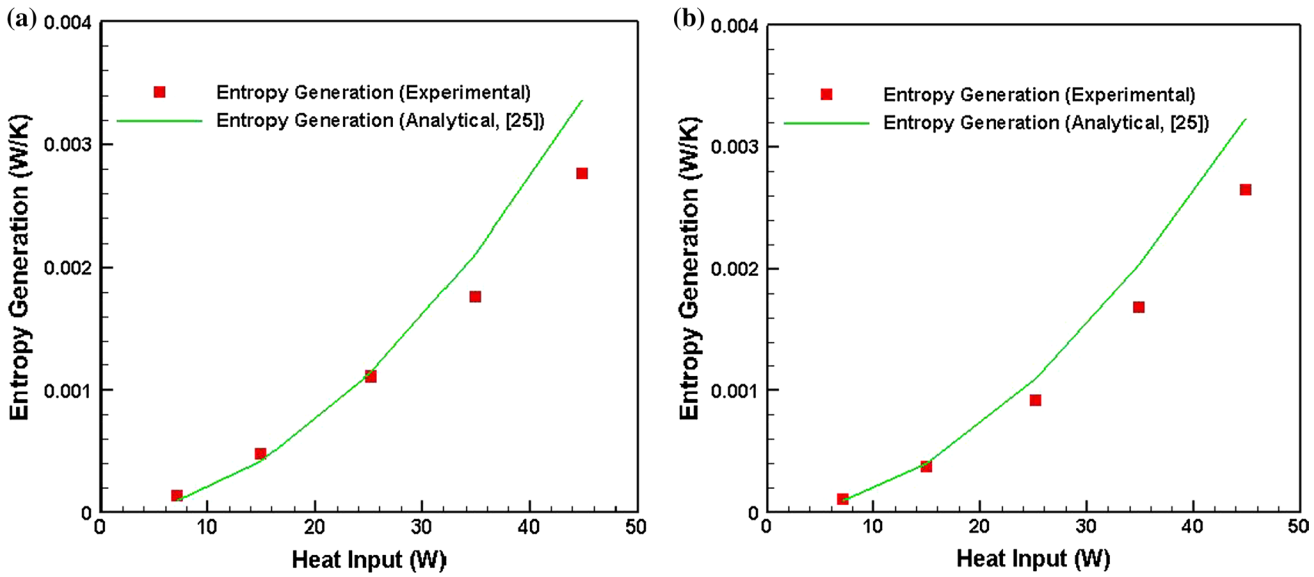


**Fig. 11** Entropy generation for heat pipes with **a** water and **b** nanofluid

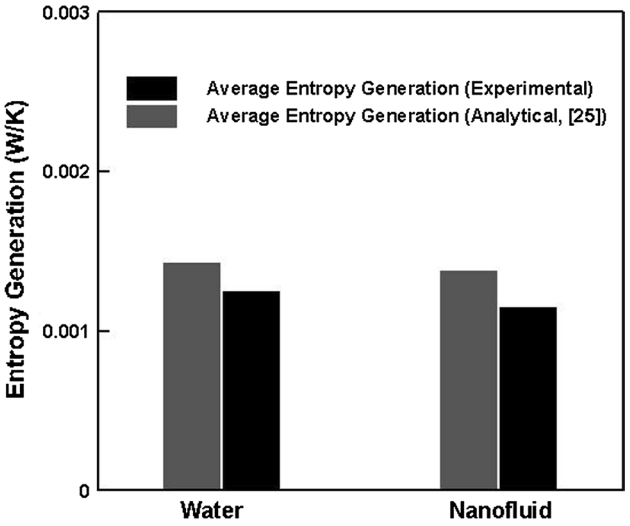


**Fig. 12** Average entropy generation of the heat pipes

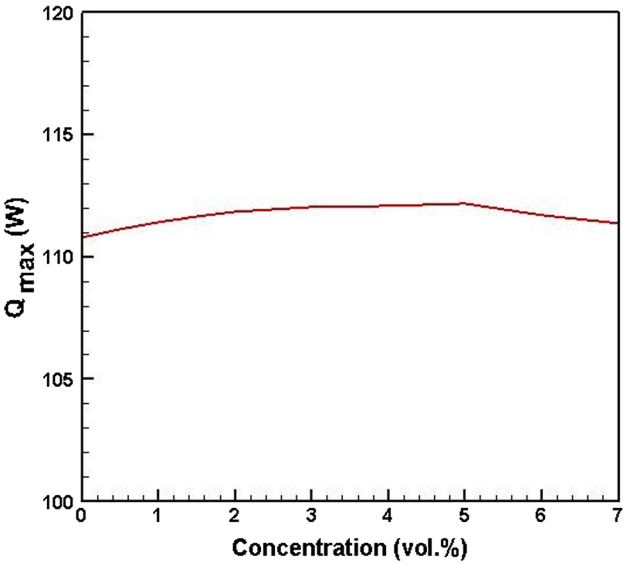


**Fig. 13** The effect of nanoparticles concentration levels on the maximum heat load

of the thermophysical properties of the nanofluid and the alteration of the characteristics of the evaporator surface at the presence of nanoparticles.

According to the results, the use of nanofluid as the working fluid of a heat pipe has influence on only a few of the partial thermal resistances. The formation of the porous layer may lead to extra thermal resistance, but may be compensated by the positive influence of the coated layer such as higher capillarity and wettability.

Also, it is logical to assume that the thermal resistance of the condenser is not affected by the nanoparticles. The reason is that the migration of the nanoparticles from the evaporator to the condenser of the heat pipe is impossible as the liquid flows from condenser to the evaporator and also the molecules of the base liquid cannot transport the nanoparticles in the vapor section. Another parameter which may have influence on the thermal resistance network of the heat pipes when using a nanofluid is the presence of the stabilizer. The evaporation and condensation of the stabilizers depend on their thermophysical properties. If the stabilizer evaporates with the working fluid it can affect the evaporation and condensation remarkably which should be taken into consideration when the influence of a nanofluid on thermal performance of a heat pipe is investigated.

## 5 Conclusions

Analytical and experimental studies were carried out to evaluate the effect of utilizing a nanofluid as the working fluid on the thermal performance of the screen mesh heat pipe. A water based $Al_2O_3$ nanofluid at a volume concentration of 1.3 % was used and the experimental results were compared with those of distilled water. The experimental results indicate that the thermal resistance of the heat pipe with a nanofluid is lower than that of the base liquid and the temperature difference between evaporator and condenser decreases as well. The experimental results were consistent with the analytical ones. The influence of the geometrical characteristics of the wick including thickness and porosity of the wick on the overall thermal resistance of the cylindrical heat pipe was also investigated. Furthermore, the thermal performance of the heat pipe was evaluated based on the second law of thermodynamics. Our results revealed that using a nanofluid as a working fluid is an efficient method to reduce the entropy generation in a heat pipe. It can be concluded that the comprehensive analytical model employed in this study is a tool for scientists to have predictions with logical validity regarding the potential of the nanofluids to improve the thermal performance of the heat pipes. The analytical model provided useful information about the liquid and vapor pressure drops and also temperature gradient along the heat pipes which can be employed before designing a heat pipes using nanofluids. Our experimental results clearly validate the analytical results and pave the way for optimized use of the provided information.

## References

1. Khanafer K, Vafai K (2011) A critical synthesis of thermophysical characteristics of nanofluids. Int J Heat Mass Transf 54:4410–4428
2. Nikkam N, Ghanbarpour M, Saleemi M, Haghighi EB, Khodabandeh R, Muhammed M, Palm B, Toprak MS (2014)

Experimental investigation on thermo-physical properties of copper/diethylene glycol nanofluids fabricated via microwave-assisted route. Appl Therm Eng 65:158–165
3. Nikkam N, Saleemi M, Haghighi EB, Ghanbarpour M, Khodabandeh R, Muhammed M, Palm B, Toprak MS (2014) Fabrication, characterization and thermo- physical property evaluation of SiC Nanofluids for heat transfer applications. Nano Micro Lett 6:178–189
4. Eastman JA, Choi SUS, Li S, Thompson LJ (1997) Enhanced thermal conductivity through the development of nanofluids. In: Proceedings of the symposium on nanophase and nanocomposite materials II, vol 457. Materials Research Society, Boston, USA, pp 3–11
5. Choi SUS, Zhang ZG, Yu W, Lockwood FE, Grulke EA (2001) Anomalous thermal conductivity enhancement in nanotube suspensions. Appl Phys Lett 79:2252–2254
6. Haghighi EB, Utomo AT, Ghanbarpour M, Zavareh A, Poth H, Khodabandeh R, Pacek A, Palm BE (2014) Experimental study on convective heat transfer of nanofluids in turbulent flow: methods of comparison of their performance. Exp Therm Fluid Sci 57:378–387
7. Utomo AT, Haghighi EB, Zavareh A, Ghanbarpourgeravi M, Poth H, Khodabandeh R, Palm B, Pacek AW (2014) The effect of nanoparticles on laminar heat transfer in a horizontal tube. Int J Heat Mass Transf 69:77–91
8. Bi J, Vafai K, Christopher DM (2015) Heat transfer characteristics and CHF prediction in nanofluid boiling. Int J Heat Mass Transf 80:256–265
9. Ghanbarpour M, Nikkam N, Khodabandeh R, Toprak MS, Muhammed M (2015) Thermal performance of screen mesh heat pipe with $Al_2O_3$ nanofluid. Exp Therm Fluid Sci 66:213–220
10. Hung YH, Teng TP, Lin BG (2013) Evaluation of the thermal performance of a heat pipe using alumina nanofluids. Exp Therm Fluid Sci 44:504–511
11. Putra N, Septiadi WN, Rahman H, Irwansyah R (2012) Thermal performance of screen mesh wick heat pipes with nanofluids. Exp Therm Fluid Sci 40:10–17
12. Moraveji MK, Razvarz S (2012) Experimental investigation of aluminum oxide nanofluid on heat pipe thermal performance. Int Commun Heat Mass Transf 39(9):1444–1448
13. Shafahi M, Bianco V, Vafai K, Manca O (2010) Thermal performance of flat-shaped heat pipes using nanofluids. Int J Heat Mass Transf 53:1438–1445
14. Teng TP, Hsu HG, Mo HE, Chen CC (2010) Thermal efficiency of heat pipe with alumina nanofluid. J Alloys Compd 504S:380–384
15. Buschmann HM (2013) Nanofluids in thermosyphons and heat pipes: overview of recent experiments and modelling approaches. Int J Therm Sci 72:1–17
16. Shang FM, Liu DY, Xian HZ, Yang YP, Du XZ (2007) Flow and heat transfer characteristics of different forms of nanometer particles in oscillating heat pipe. J Chem Indust Eng 58:2200–2204
17. Liu ZH, Zhu QZ (2011) Application of aqueous nanofluids in a horizontal mesh heat pipe. Energ Convers Manage 52:292–300
18. Wang GS, Song B, Liu ZH (2010) Operation characteristics of cylindrical miniature grooved heat pipe using aqueous CuO nanofluids. Exp Therm Fluid Sci 34:1415–1421
19. Asirvatham LG, Nimmagadda R, Wongwises S (2013) Heat transfer performance of screen mesh wick heat pipes using silver–water nanofluid. Int J Heat Mass Transf 60:201–209
20. Do KH, Ha HJ, Jang SP (2010) Thermal resistance of screen mesh wick heat pipes using the water-based $Al_2O_3$ nanofluids. Int J Heat Mass Transf 53:5888–5894
21. Huminic G, Huminic A (2011) Heat transfer characteristics of a two-phase closed thermosyphons using nanofluids. Exp Therm Fluid Sci 35:550–557
22. Naphon P, Assadamongkol P, Borirak T (2008) Experimental investigation of titanium nanofluids on the heat pipe thermal efficiency. Int Commun Heat Mass Transf 35:1316–1319
23. Gunnasegaran P, Abdullah MZ, Shuaib NH (2013) Influence of nanofluid on heat transfer in a loop heat pipe. Int Commun Heat Mass Transf 47:82–91
24. Zhu N, Vafai K (1999) Analysis of cylindrical heat pipes incorporating the effects of liquid-vapor coupling and non-Darcian transport-a closed form solution. Int J Heat Mass Transf 42:3405–3418
25. Shafahi M, Bianco V, Vafai K, Manca O (2010) An investigation of the thermal performance of cylindrical heat pipes using nanofluids. Int J Heat Mass Transf 53:376–383
26. Bejan A (1982) Entropy Generation Through Heat and Fluid Flow. Wiley, New York
27. Ghanbarpour M, Khodabandeh R (2015) Entropy generation analysis of cylindrical heat pipe using nanofluid. Thermochim Acta 610:37–46
28. Park MK, Boo JH (2012) Thermal performance of a heat pipe with two dissimilar condensers for a medium-temperature thermal storage system. J Appl Sci Eng 15:123–129
29. Ghanbarpour M, Bitaraf Haghigi E, Khodabandeh R (2014) Thermal properties and rheological behavior of water based $Al_2O_3$ nanofluid as a heat transfer fluid. Exp Therm Fluid Sci 53:227–235
30. Ghanbarpour M, Nikkam N, Khodabandeh R, Toprak MS (2015) Thermal performance of inclined screen mesh heat pipes using silver nanofluid. Int Commun Heat Mass Transf 67:14–20